NASA Contractor Report 4030

Structural Properties of Bismuth-Bearing Semiconductor Alloys

Martha A. Berding, A. Sher,
and A.-B. Chen

CONTRACT NAS1-18180
DECEMBER 1986

(NASA-CR-4030) STRUCTURAL PROPERTIES OF BISMUTH-BEARING SEMICONDUCTOR ALLOYS Final Report (SRI International Corp.) 38 p CSCL 46D

N87-14170

Unclas
H1/76 43957

NASA

NASA Contractor Report 4030

Structural Properties of Bismuth-Bearing Semiconductor Alloys

Martha A. Berding and A. Sher
SRI International
Menlo Park, California

A.-B. Chen
Auburn University
Auburn, Alabama

Prepared for
Langley Research Center
under Contract NAS1-18180

NASA
National Aeronautics
and Space Administration

Scientific and Technical
Information Branch

1986

CONTENTS

LIST OF ILLUSTRATIONS v

LIST OF TABLES vii

I INTRODUCTION 1

II TECHNICAL DISCUSSION 3

A. Task 1—Literature Search 3

B. Task 2—Bond Energies, Bond Lengths, and Strain Coefficients for Pure Compounds 3

C. Task 3—Bond Energies, Bond Lengths, and Strain Coefficients for Alloys 6

D. Task 4—Mixing Enthalpy, Miscibility Gaps, and Critical Temperatures 8

E. Task 5—Cluster Formation 12

F. Task 6—Semiconductor Hardness 15

G. Task 7—Vacancy Formation Energy 26

III CONCLUSIONS 31

REFERENCES 33

PRECEDING PAGE BLANK NOT FILMED

ILLUSTRATIONS

1 Tetrahedral Cluster Types 13

2 Cluster Energies as a Function of Concentration for InSbBi 14

3 Deviations of Cluster Populations from a Random Distribution as a Function of Concentration for InSbBi 16

4 Alloy Bond Lengths as a Function of Concentration for InSbBi 19

5 Mixing Free Energies as a Function of Concentration for InSbBi 20

6 Cluster Energies as a Function of Concentration for InAsBi 21

7 Deviations of Cluster Populations from Random Distributions as a Function of Concentration for InAsBi 22

8 Alloy Bond Lengths as a Function of Concentration for InAsBi 23

9 Mixing Free Energy as a Function of Concentration for InAsBi 24

PRECEDING PAGE BLANK NOT FILMED

TABLES

1 Compound Bond Lengths and Bond Energies 4

2 Calculated and Experimental Elastic Constants 7

3 Elastic Constant Scaling Factors 7

4 Alloy Impurity Bond Lengths 9

5 Alloy Excess Bond Energy 9

6 Mixing Enthalpy Parameter Ω for Bismuth Zincblende Alloys 10

7 Critical Temperature, T_c, Melting Temperature, T_m, Lattice Mismatch Parameter, δ_o, and the Ratio $|\delta_o|/\delta_m$ 11

8 Hardness Values of Semiconductors 25

9 Vacancy Formation Energies for Bi Compounds and Other Group IV, III-V, and II-VI Compounds 29

PRECEDING PAGE BLANK NOT FILMED

I INTRODUCTION

This is the final report on SRI Project 1452 under NASA contract NAS1-18180 to investigate the structural properties of bismuth-bearing semiconducting alloys.

Although the III-V bismuth compounds do not crystallize in zincblende structures, if such compounds could be grown, they would be expected to have semimetallic properties. When they are alloyed with positive-band-gap III-V compounds, they should produce narrow, positive-gap semiconductors, which would be candidates for use in infrared detection devices. Current materials with such narrow band gaps have notoriously poor structural properties. The purpose of this investigation has been to determine whether the structural properties of the bismuth-bearing alloys appear to justify a major program to grow them. To this end, we have calculated the structural properties expected for the bismuth-bearing alloys; the anion-substituted alloys $InSb_{1-x}Bi_x$, $InAs_{1-x}Bi_x$, and $InP_{1-x}Bi_x$; and the cation-substituted alloys $Ga_{1-x}In_xBi$, $Al_{1-x}In_xBi$, and $Al_{1-x}Ga_xBi$.

This report is organized according to items on the research task list of the contract:

Task 1: Conduct a literature search designed to gather the input parameters needed to calculate the structural properties of the Bi-bearing alloys $InSb_{1-x}Bi_x$, $InAs_{1-x}Bi_x$, $InP_{1-x}Bi_x$, $Ga_{1-x}In_xBi$, $Al_{1-x}In_xBi$, $Al_{1-x}Ga_xBi$.

Task 2: Calculate the bond energies, bond lengths, and strain coefficients for the pure compounds AlBi, GaBi, and InBi.

Task 3: Use the results of Task 2 and similar information already at SRI's disposal for other compounds to calculate bond length, bond energy, and strain coefficient modifications occurring in the alloys.

Task 4: Calculate the mixing enthalpy for the Bi-bearing alloys; then predict miscibility gaps and critical metastable-to-stable material transi-temperatures.

Task 5: Calculate tendencies toward micro- and macro-cluster formation.

Task 6: Calculate the hardness of the alloys listed in Task 1.

Task 7: Calculate vacancy formation energies.

Task 8: Prepare and submit reports.

II TECHNICAL DISCUSSION

A. *Task 1—Literature Search*

SRI conducted a literature search to determine the current status of research concerning the growth of bismuth-bearing alloys and to gather the needed input parameters for theoretical calculations.

We found reports of the growth of only one bismuth-bearing zincblende alloy in the literature (Jean-Louis and Hamon, 1969a,b; Joukoff and Jean-Louis, 1972; Oe et al., 1981; Noreika et al., 1982, 1983). Using equilibrium growth methods, $InSb_{1-x}Bi_x$ alloys were grown with up to ~ 2.6 mole percent bismuth, the solid-solubility limit of InBi in InSb. Metastable solid solutions of $InSb_{1-x}Bi_x$ were grown by Zilko and Green (1978; 1980); up to 12 mole percent InBi was incorporated into InSb, with the semimetal-semiconductor transition occurring at ~ 11 mole percent at 20 K. They found the metastable $InSb_{1-x}Bi_x$ to have good temporal and thermal stability against phase separation.

The primary parameters used in the theoretical calculations of the structural properties of the Bi-bearing alloys are the atomic energy levels of the constituents and the bismuth zincblende-compound bond lengths. None of the bismuth compounds crystalize in a zincblende structure; the only binary compound reported in the literature is InBi, which forms a tetragonal structure similar to PbO (Wykoff, 1963). Thus, no experimental values were available for the tetrahedral bond lengths for AlBi, GaBi, and InBi. In addition, no measurements were found reported in the literature of the properties studied theoretically here, e.g. hardness, bond energies, and vacancy formation energies.

B. *Task 2—Bond Energies, Bond Lengths, and Strain Coefficients for Pure Compounds*

Although AlBi, GaBi, and InBi do not form zincblende structures, the tetrahedral bond lengths for these compounds are a necessary input to the alloy structural calculations. Because no experimental bond lengths are available, SRI determined the zincblende bond lengths theoretically. Throughout this report, we refer to the zincblende bond lengths of InBi, GaBi, and AlBi, although the materials described by these bond lengths have never been grown. For the anion-substituted alloys, $InA_{1-x}Bi_x$ where A = P, As, or Sb, the bond lengths are perhaps most accurately interpreted as the limit of the zincblende alloy bond length as the concentration, x, approaches 1.

The experimental data for $InSb_{1-x}Bi_x$ with $x < 0.03$ (Joukoff and Jean-Louis, 1972) were used to extrapolate the bond length of zincblende InBi, assuming Vegard's law holds; that is, that the alloy bond length varies linearly with concentration. The bond lengths of InP, InAs, InSb, InBi, GaBi, and AlBi were computed by two methods. First, SRI used Pauling covalent

PRECEDING PAGE BLANK NOT FILMED

radii (R) and known III-V compound bond lengths (including the InBi bond length extrapolated from the alloy data) to deduce Bi and cation covalent radii. From these radii, the compound bond lengths, d, were computed from

$$d = R(\text{cation}) + R(\text{anion}).$$

Second, SRI used Harrison's theory (Harrison, 1980; 1983) to predict zincblende bond lengths. For compounds of known bond lengths, this theory yields exact agreement with experiment, because the model incorporates the experimental bond lengths into the determination of the repulsive overlap energy, V_0. For GaBi and AlBi compounds with unknown bond lengths, appropriately averaged coefficients were used in the calculation of V_0. Calculated bond lengths are summarized in Table 1. Note that the bond lengths calculated from covalent radii and Harrison's model give agreement within 2 percent.

Table 1

COMPOUND BOND LENGTHS AND BOND ENERGIES

Compound	Bond Length (Å)			Bond Energy (eV)		
	Experiment	Covalent Radii	Harrison's Theory	Experiment	Harrison's Theory	Current Work
InP	2.54	2.51	2.54	-1.74	-2.05	-1.98
InAs	2.62	2.62	2.61	-1.55	-1.72	-1.58
InSb	2.81	2.82	2.81	-1.40	-1.24	-1.00
InBi	2.88*	2.88	2.88	+	-1.16	-0.53
GaBi	+	2.72	2.68	+	-1.47	-0.87
AlBi	+	2.71	2.72	+	-1.60	-1.02
ZnTe				-1.20	-1.03	-0.87
CdTe				-1.10	-0.96	-0.81
HgTe				-0.82	-0.48	-0.32

*Extrapolated from the $InSb_{1-x}Bi_x$ alloy bond lengths.
+No experimental values available.

Bond energies were computed from Harrison's model, using the zincblende bond lengths calculated above. The bond energy is given by (Sher et al., 1985a)

$$E_b = 2\varepsilon_b + 2(\varepsilon_{met}{}^{a} + \varepsilon_{met}{}^{b}) + V_0 + E_{tr} + E_{pro}{}^{a} + E_{pro}{}^{c} \quad , \tag{1}$$

where ε_b is the bond formation energy; $\varepsilon_{met}{}^a$ and $\varepsilon_{met}{}^c$ are the metallization energies from coupling through the anion and cation sites, respectively; V_0 is the repulsive overlap energy;

$$E_{tr} = n(\varepsilon_p{}^c - \varepsilon_p{}^a)/4 \tag{2}$$

$$n = \begin{cases} 0 & \text{for group IV compounds} \\ 1 & \text{for III-V compounds} \\ 2 & \text{for II-VI compounds} \end{cases}$$

is the energy per bond necessary to transfer n electrons from an anion to a cation site, where $\varepsilon_s{}^a$, $\varepsilon_p{}^a$, $\varepsilon_s{}^c$, and $\varepsilon_p{}^c$ are atomic term values; and

$$E_{pro}{}^{a(c)} = [\varepsilon_p{}^{a(c)} - \varepsilon_p{}^{a(c)}]/4 \tag{3}$$

is the promotion energy per bond to form sp^3 hybrids on the anion (cation) site.

SRI computed atomic term values from an ab-initio total energy calculation based on pseudo-potentials (Bachelet et al., 1982). These calculations include the spin-orbit (SO) interaction, so that the degeneracy of the p-levels is partially removed. The p-levels are split into a deeper singly degenerate state with total angular momentum J = 1/2 and with atomic term value $\varepsilon_{p1/2}$, and a shallower two-fold degenerate J = 3/2 state, with $\varepsilon_{p3/2}$. This p-level splitting will have an important effect on the properties considered below and is especially important for the heavier atoms such as bismuth, where this relativistic correction is significant. Harrison's model discussed above does not include this SO splitting into the calculation of the bond energy. It is the last three terms in Eq. (1) which are modified by the inclusion of the SO splitting in the calculation. With SO splitting included, the transfer energy becomes

$$E_{tr} = n(\varepsilon_{p1/2}{}^c - \varepsilon_{p3/2}{}^a) \quad , \tag{4}$$

with n as given in Eq. (2), and the promotion energy is given by

$$E_{pro}{}^{a(c)} = [2\varepsilon_{p3/2}{}^{a(c)} - \varepsilon_s{}^{a(c)} - \varepsilon_{p1/2}{}^{a(c)}] \quad . \tag{5}$$

In Table 1, we see that the effect of including the SO splitting in the calculations is significant, especially for the compounds containing heavier atoms and results in as much as a 54 percent reduction in the magnitude of the bond energy for the Bi compounds. The large SO splitting in Bi, along with the other effects of the relativistic terms which cause a reduction of the s-state energies, is likely to explain why bismuth compounds do not tend to form in tetrahedrally coordinated structures, since it is so costly to promote electrons to form sp^3 hybrids.

Shown for comparison in Table 1 are the bond energies of three II-VI compounds: ZnTe, CdTe, and HgTe. Compared to these compounds, which form narrow-gap II-VI alloys, the bismuth compounds and their alloys are expected to be more strongly bonded.

SRI computed the elastic constants using Harrison's model for bonding in cubic semiconductors. The bulk modulus, B, $C_{11} - C_{12}$, and C_{44} can be determined by application of a uniform volume expansion, a shear deformation and a graphite distortion, respectively, to the zincblende structure (Harrison, 1980; 1983; Chen and Sher, 1983). The calculated elastic constants for the six compounds of interest here are given in Table 2. Although the quantitative agreement with the experimental values is poor, in particular for the bulk modulus, which indicates a need for improvement in the theoretical model used, the trends among compounds is properly predicted.

One way in which to improve the quantitative agreement with the experimental elastic constants is through a uniform scaling of the theoretical values. SRI determined scaling factors for B, $C_{11} - C_{12}$, and C_{44} by a least squares fit to all of the III-V compounds with experimentally known elastic constants. The three scaling constants obtained and the maximum resulting error for any one compound (compared with experiment) are summarized in Table 3.

SRI also calculated the bond-stretching and bond-bending force constants α and β for the zincblende structures using the Valence Force Field (VFF) model, discussed by Keating (1966) and Martin (1970). Scaled elastic constants were used; the results are summarized in Table 2.

The elastic constants calculated for the hypothetical zincblende Bi compounds are larger than the corresponding experimental values for the Te compounds currently used in infrared detectors. Alloying these Bi compounds with some of the others listed in Table 1 could produce a fairly strong and resilient material.

C. *Task 3—Bond Energies, Bond Lengths, and Strain Coefficients for Alloys*

SRI calculated local bond length and bond energy modifications expected in the dilute alloys using a perturbation-expansion form of Harrison's theory as discussed by Chen and Sher (1985a). This formalism permits the inclusion of chemical effects on the bond length shifts as well as the bond strain terms of the Valence Force Field (VFF) model (Keating, 1966). In addition, the perturbation expansion formalism permits the use of measured or theoretical strain coefficients in the VFF, thus avoiding the inadequacy of Harrison's theory in predicting the elastic constants accurately.

By treating the dilute species as an impurity in the host lattice, SRI calculated impurity bond lengths and excess bond energies using the scaled theoretical force constants and strain coefficients. For an alloy $A_xB_{1-x}C$ with $x \ll 1$, the excess bond energy, ΔE, is defined as the extra energy per bond required for the impurity substitution over and above the binding-energy difference between the BC and AC crystals. The binding-energy difference accounts for much of the substitution energy; however, the correction measured by the excess energy can be significant. This excess energy results from strain energies and chemically driven charge redistributions around the defect. Several valence force field models were used to calculate the

Table 2

CALCULATED AND EXPERIMENTAL ELASTIC CONSTANTS
(All values 10^{11} dynes/cm^2 unless otherwise noted)

Compound	B			C_{11}-C_{12}			C_{44}				
	Experimental	Theory	Scaled Theory	Experimental	Theory	Scaled Theory	Experimental	Theory	Scaled Theory	α^* (N/m)	β^* (N/m)
InP	7.25	2.84	6.24	4.46	4.41	5.10	4.60	3.41	4.88	34.1	7.49
InAs	5.80	2.62	5.77	3.80	3.79	4.38	3.96	2.91	4.18	32.7	6.63
InSb	4.66	1.96	4.30	3.02	2.73	3.16	3.02	2.08	2.98	26.2	5.12
InBi	—	1.81	3.99	—	2.34	2.71	—	1.82	2.61	25.0	4.51
GaBi	—	2.01	4.42	—	3.15	3.64	—	2.51	3.60	25.7	5.67
AlBi	—	2.14	4.71	—	3.16	3.65	—	2.45	3.51	27.7	5.72
ZnTe	5.09	2.10	—	3.06	3.47	—	3.12	2.80	—	29.4	4.66
CdTe	4.24	1.41	—	1.68	2.47	—	1.99	2.10	—	26.6	2.72
HgTe	4.22	1.69	—	1.70	2.61	—	2.11	2.10	—	26.4	2.75

*Calculated using the scaled theory elastic constants for the III-V compounds and the experimental elastic constants for the II-VI compounds.

Table 3

ELASTIC CONSTANT SCALING FACTORS

Constant	Scaling Constant	Maximum Error (percent)
B	2.20	14
C_{11}-C_{12}	1.16	15
C_{44}	1.43	7

bond length and bond energy modifications occurring in dilute alloys, as discussed in Sher et al. (1985a): model C is a simple spring model where the bond bending force constants, β, are set to zero and the second-shell atoms are connected to a fixed boundary; model FPT is the full perturbation theory of Chen and Sher (1985a) with a continuum connected to the second-shell atoms; and model D2 is the FPT with all of the chemical terms neglected. Resulting bond lengths and energy modifications using these three models are summarized in Tables 4 and 5.

The bond length changes for the impurity species is from 20 to 35 percent of the bond length differences between the impurity and host bond lengths, with all impurity bond lengths shifting toward the host bond length. Thus, the impurity bond lengths are nearer the bond lengths of the impurity compound than those of the host compound. The full perturbation theory (FPT) results differ from model D2, which is the full perturbation theory without the chemical terms, by no more than 0.003 Å for all the alloys studied, far less than the experimental accuracy of the extended X-ray absorption fine structure (EXAFS) measurements used to determine alloy bond length shifts.

The excess bond energy is greatest in the (P,Bi)In alloy, primarily because of the large strains resulting from the large bond lengths difference between InP and InB (approximately 13 percent). The bond energy shifts due to the chemical terms in the FPT are also most significant for this system. For the nearly lattice matched system (Ga,Al)Bi, the bond excess energies are negligible.

SRI began work on the alloy variations of the strain coefficients, although we have not yet made final predictions for the bismuth-bearing alloys. We expect that the dependence on the concentration is not a simple VCA dependence, but rather will exhibit an upward bowing, as does the hardness. The idea proposed previously of modifying Harrison's theory by introducing a new scaling law for the bonding energy and the repulsive energies, and thereby obtaining the correct strain coefficients from the theory directly, lends itself to the prediction of the alloy strain coefficients. But such a calculation depends on knowing the elastic constants *a priori*, because it is from these that the scaling laws are determined for a given compound. Thus, we cannot determine the dependence of the strain coefficients on the concentration, x, in this manner for the bismuth compounds because the elastic constants of these compounds have not been experimentally determined.

D. *Task 4—Mixing Enthalpy, Miscibility Gaps, and Critical Temperatures*

SRI computed the dilute alloy mixing enthalpy as discussed by Chen and Sher (1985a). For modest pressures, the entropy term in the Helmholtz free energy can be neglected, giving, for an alloy $A_xB_{1-x}C$,

$$\Delta H_m = \Delta E_m = E_{alloy} - [xE_{AC} + (1-x)E_{BC}] \quad , \tag{6}$$

Table 4

ALLOY IMPURITY BOND LENGTHS (Å)

Compound		Bond Lengths				
Impurity	Host	Impurity	Host	C	D2	FPT
InBi	InP	2.880	2.541	2.774	2.762	2.761
InP	InBi	2.541	2.880	2.608	2.607	2.607
InBi	InAs	2.880	2.622	2.802	2.796	2.796
InAs	InBi	2.622	2.880	2.674	2.674	2.675
InBi	InSb	2.880	2.805	2.861	2.860	2.859
InSb	InBi	2.805	2.880	2.823	2.823	2.823
InBi	GaBi	2.880	2.700	2.834	2.828	2.825
GaBi	InBi	2.700	2.880	2.744	2.744	2.746
InBi	AlBi	2.880	2.715	2.836	2.832	2.830
AlBi	InBi	2.715	2.880	2.753	2.753	2.755
GaBi	AlBi	2.700	2.715	2.704	2.704	2.705
AlBi	GaBi	2.715	2.700	2.711	2.711	2.710

Table 5

ALLOY EXCESS BOND ENERGY
(kcal/mole-band)

		Model		
Impurity	Host	C	D2	FPT
InBi	InP	1.939	2.294	2.326
InP	InBi	1.663	1.760	1.800
InBi	InAs	1.091	1.235	1.254
InAs	InBi	0.955	1.010	1.035
InBi	InSb	0.079	0.087	0.089
InSb	InBi	0.077	0.081	0.083
InBi	GaBi	0.446	0.538	0.543
GaBi	InBi	0.440	0.467	0.462
InBi	AlBi	0.396	0.456	0.463
AlBi	InBi	0.377	0.399	0.405
GaBi	AlBi	0.003	0.004	0.002
AlBi	GaBi	0.003	0.004	0.002

where ΔH_m is the mixing enthalpy and ΔE_m is the mixing energy. Equation (6) can be rewritten in terms of the excess free energy per bond, ΔE, computed above and summarized in Table 5:

$$\Delta H_m = x(1-x)\Omega \quad , \tag{7}$$

$$\Omega = 2[\Delta E(A \text{ in } BC) + \Delta E(B \text{ in } AC)] \quad , \tag{8}$$

where Ω is the mixing enthalpy parameter. From Eq. (7) ΔH_m should be viewed as a lower bound on the mixing enthalpy, because measured mixing enthalpies will, in general, be affected by contributions from nonideal structures such as vacancies, impurities, dislocations, grain boundaries, and surface conditions.

Calculated Ω for the various bismuth zincblende compounds are summarized in Table 6. We see that the mixing enthalpy parameter is positive for all of the bismuth-bearing alloys, indicating possible miscibility gaps for all alloys. The mixing enthalpy is lowest for $InBi_xSb_{1-x}$ and $Ga_xAl_{1-x}Bi$ alloys, which have the smallest lattice mismatch of the constituent compounds, while the mixing enthalpy is largest for $InBi_xP_{1-x}$, which has the largest compound bond length mismatch of the alloys considered.

Table 6

MIXING ENTHALPY PARAMETER Ω
FOR BISMUTH ZINCBLENDE ALLOYS
(kcal/mole)

	Model		
Compound	C	D2	FPT
(BiP)In	7.20	8.11	8.25
(BiAs)In	4.09	4.49	4.58
(BiSb)In	0.31	0.34	0.34
(InGa)Bi	1.77	2.10	2.01
(InA1)Bi	1.55	1.71	1.74
(GaA1)Bi	0.01	0.02	0.01

From the mixing enthalpies, we can obtain an estimate of the miscibility of the zincblende alloys. In a truly random alloy, the criteria for alloy mixing at a temperature, T, is that $T \geq T_c$, where the critical temperature, T_c, is given by $\Omega/(2R_g)$, where R_g is the universal gas

constant. For complete miscibility throughout the entire concentration range, the requirement is that the melting temperature of both the pure compounds of the alloys be greater than T_c,

$$\frac{T_m}{T_c} > 1 \quad , \tag{9}$$

where T_m is the lower melting temperature of the constituent compounds. Values of T_c for the bismuth alloys and the ratio T_m/T_c are summarized in Table 7.

Table 7

CRITICAL TEMPERATURE, T_c, MELTING TEMPERATURE, T_m,
LATTICE MISMATCH PARAMETER, δ_0,
AND THE RATIO $|\delta_0|/\delta_m$

Compound	$\|\delta_0\|$ (percent)	T_c (K)	T_m (K)*	T_m/T_c	$\|\delta_0\|/\delta_m$
(BiP)In	13.3	2080	1343	0.65	0.10
(BiAs)In	9.0	1150	1215	1.06	0.10
(BiSb)In	2.7	87	798	9.17	0.08
(InGa)Bi	6.2	500	—	—	—
(InA1)Bi	5.7	440	—	—	—
(GaAl)Bi	0.5	2	—	—	—

*American Institute of Physics (1972). T_m is the melting temperature of the nonbismuth compound.

Perhaps a better rule for miscibility (Chen and Sher, 1985a) is

$$|\delta_0|/\delta_m < 1 \tag{10}$$

where

$$\delta_m = 1.63\ \chi_m \tag{11}$$

and χ_m is the ratio of the rms bond-length amplitude fluctuation to the bond length at the melting temperature, T_m. The lattice mismatch parameter, δ_0, is given by

$$\delta_0 = 1 - d(\text{impurity})/d \quad . \tag{12}$$

Values of the ratio $|\delta_0|/\delta_m$ are summarized in Table 7.

For both of the above criteria for miscibility, the relevant melting temperature is the lower of the two compound melting temperatures. No experimental melting temperatures are available for the zincblende bismuth compounds. Thus in the above calculations, SRI assumed that the relevant temperature was that of the nonbismuth compound, thereby implying that the melting temperature of the bismuth compounds are the higher of the two. From Table 7, we see that first criterion for miscibility $T_m/T_c > 1$ is satisfied for the two anion-substituted zincblende alloys (BiAs)In and (BiSb)In, and that a miscibility gap is predicted for zincblende (BiP)In. We have not made miscibility predictions for the cation-substituted alloys having a common bismuth anion since no zincblende melting temperatures are available for the bismuth compounds. The second criterion for miscibility $|\delta_0|/\delta_m < 1$ is satisfied for all three of the anion-substituted alloys.

Of the three anion-substituted alloys, InSbBi shows the least tendency toward spinoidal decomposition (see Table 7). In addition, the assumption that T_m of zincblende InBi be greater than T_m of the other indium compound is the least stringent for InSbBi, with T_m(InSb) = 798 K, the strictest requirement for miscibility being that T_m(InBi) > T_c = 87 K. The low critical temperature of the alloy, InSbBi, indicate that this material will be miscible for temperatures near 300 K. In contrast, the high critical temperature of InAsBi and the ratio of T_m/T_c close to unity indicate a narrow miscibility range at a temperature (~ 1200 K) far from room temperature.

Our interpretation of the above results on miscibility is necessarily somewhat tentative. In the miscibility calculations, we have assumed that no allotropic phase transitions occur, that the constituent compounds form zincblende structures throughout the entire temperature and composition range. This is known not to be the case for the bismuth-bearing alloys, because the bismuth compounds themselves are not known to form zincblende structures. Thus, the above miscibility criterion should be used in conjunction with information on the allotropic phase transitions to correctly predict miscibility.

E. *Task 5—Cluster Formation*

SRI has generalized the above theory of dilute alloys to concentrated alloys using statistics based on combinations of tetrahedral clusters of five atoms (Chen and Sher, 1985b). This generalization is based on an extension of the regular solution theory based on pair energies to a theory for five-atom clusters. For an alloy $A_xB_{1-x}C$, the building blocks are clusters of $A_mB_{4-m}C$, where m ranges from 0 to 4, as shown in Figure 1. Effective cluster energies, e, and local bond lengths can then be computed for each of the cluster types. The partition function, Z, that is obtained yields the mixing Helmholtz free energy, ΔF. A measure of the deviations from randomness, δx, is given by

$$\delta x = x_m - x_m^{(0)} \quad , \tag{13}$$

where x_m is the cluster distribution, $x_m^{(0)}$ is the corresponding value for a random alloy,

$$x_m^{(0)} = (g_m)x^m \, 1-x^{4-m} \quad , \tag{14}$$

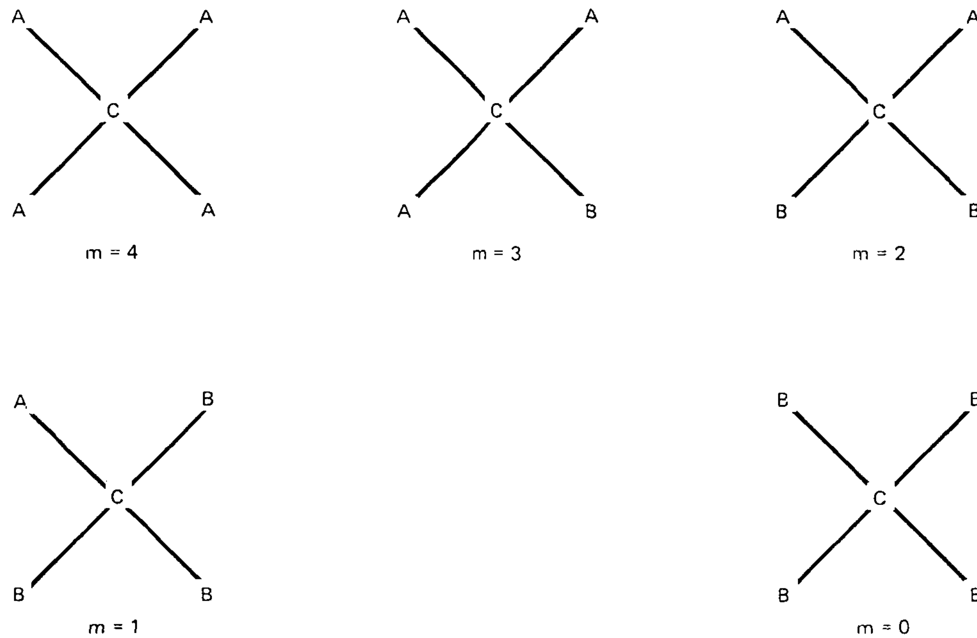

FIGURE 1 TETRAHEDRAL CLUSTER TYPES

and g_m is the cluster degeneracy

$$g_m = \begin{matrix} 1 & m=0,4 \\ 4 & m=1,3 \\ 6 & m=2 \end{matrix} \qquad (15)$$

For the truly random alloy, $\delta x = 0$ and, no micro- or macroclustering is expected to occur.

The results of SRI's microcluster calculations for InSbBi and InAsBi are summarized below. As discussed above, the cation-substituted alloys appear to be the most likely candidates for device materials, and these two alloys serve to illustrate the problems associated with the structural properties of bismuth-bearing alloys.

The effective energies of various five-atom clusters for InBiSb are shown in Figure 2. The energy for the cluster which contains four Bi and one In atoms, Sb(0)Bi(4), is e_4; e_3 is

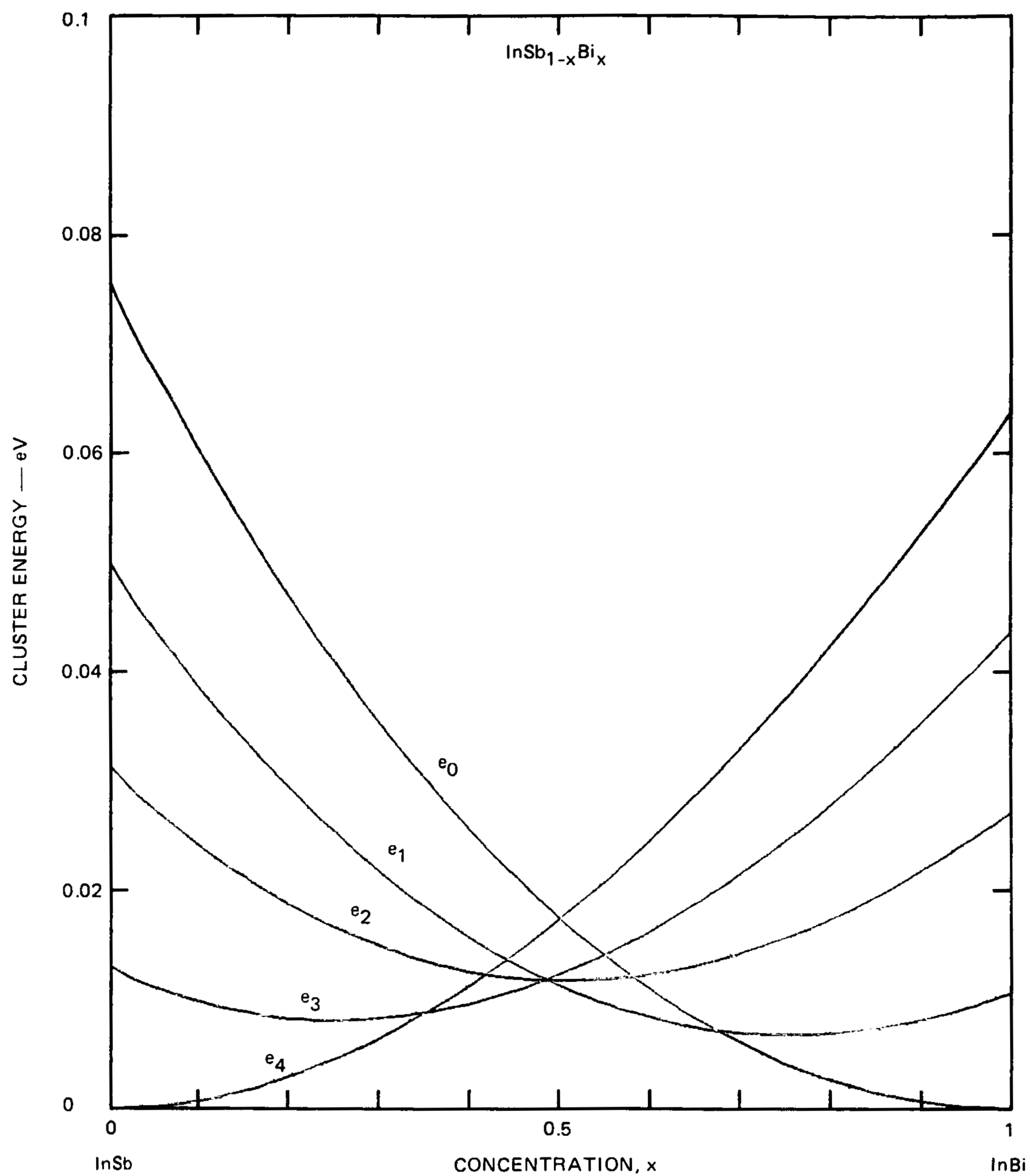

FIGURE 2 CLUSTER ENERGIES AS A FUNCTION OF CONCENTRATION FOR InSbBi

the energy for the cluster InSb(1)Bi(3); and so on. Only the nonlinear dependence of the energy on the number of atoms of either species in the cluster is responsible for the nonrandom distribution. The δ shown in Figure 3 are these nonlinear energies, defined as

$$\delta_3 = e_3 - (3e_4 + e_0)/4 \quad ,$$

$$\delta_2 = e_2 - (e_4 + e_0)/2$$

and

$$\delta_1 = e_1 - (e_4 - 3e_0)/4$$

for 78 K, 300 K, and 600 K. The reference energy $\Delta = xe_4 + (1-x)e_0$ is important and has been included in the calculation of the mixing free energies. The energies shown in Figure 3 indicate that InSbBi would be a rather innocent alloy if the zincblende structure were the lowest-energy structure. Indeed, the deviations from randomness shown in Figure 3 indicate that the zincblende alloy should be very close to a random alloy at 78, 300, and 600 K. Figure 4 shows that the bond lengths vary smoothly with concentration x.

According to the mixing free energy, ΔF (shown in Figure 5), miscibility should not be a problem if InBi behaved like a zincblende compound. This result is consistent with the results obtained for the dilute alloy limit discussed in Task 4 above. In reality, InBi has a tetragonal structure similar to PbO (Wykoff, 1963). The only clue that Bi behaves differently from other group V atoms is that Bi has a much larger spin-orbit splitting ($\varepsilon_{p3/2} - \varepsilon_{p1/2} > 2$eV).

SRI repeated the above calculations for InAsBi; the results are summarized in Figures 6 through 9. Because the estimated bond length of InBi is much larger than that of InAs and the strain energy is the dominant contribution to the mixing energy (especially true for anion-substituted alloys), large cluster energies emerge. However, the nonlinear parts are only about one-tenth the magnitude of the e′. The mixing free energies, ΔF (shown in Figure 9), show that InBi and InAs are hard to mix, even without considering structures other than zincblende, again consistent with the dilute alloy results. Figure 8 shows that the bond length associated with a given bond at a given concentration is not very sensitive to the different clusters. This result is common to all the III-V pseudo-binary alloys and is also consistent with the available EXAFS data.

F. *Task 6—Semiconductor Hardness*

SRI calculated hardness values for the bismuth compounds using a hardness model discussed by Sher et al. (1985b). In this model, the Vicker's hardness is found to be dominated by the interaction energy of the dislocations generated by the indentation. Contributions to the

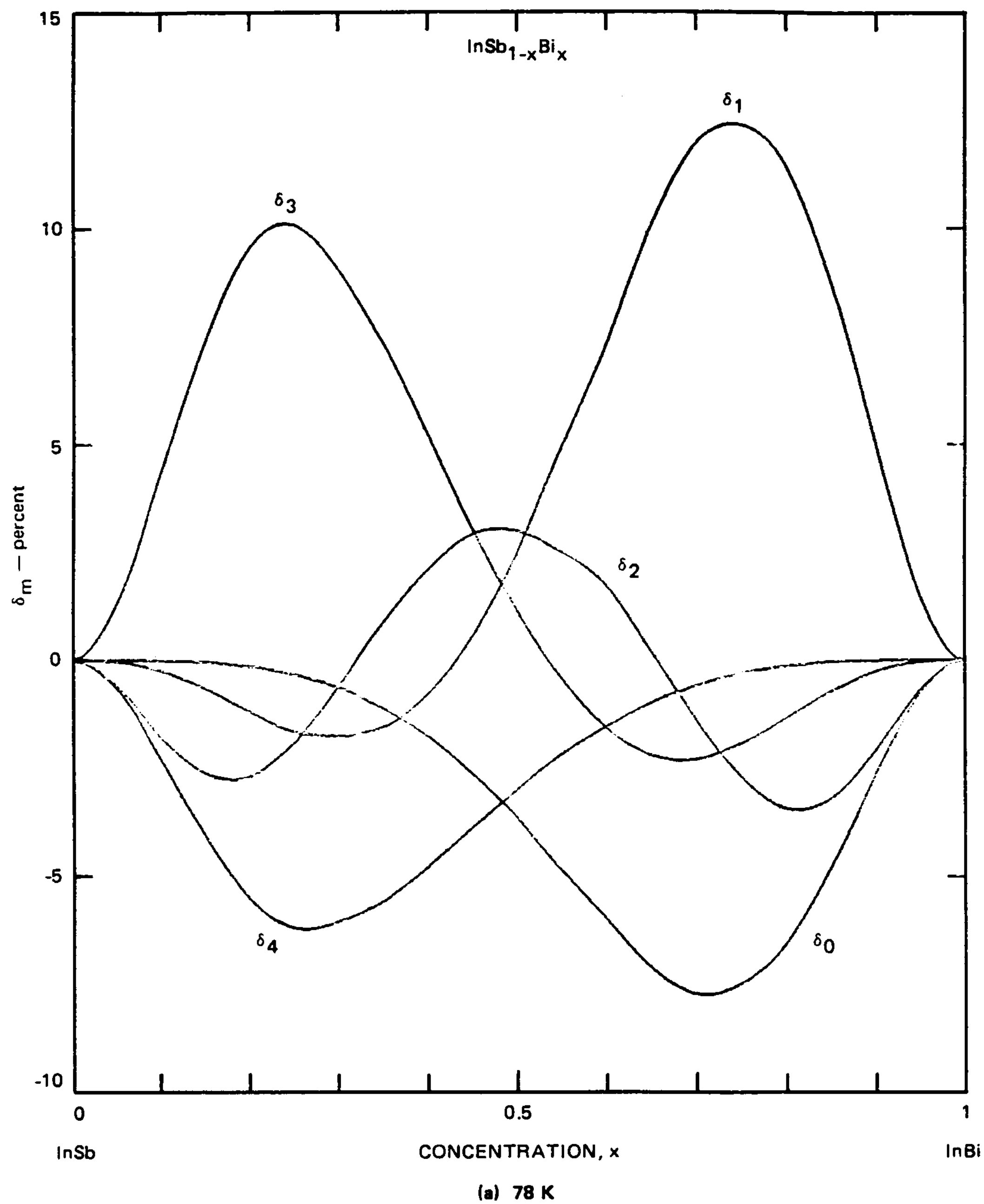

(a) 78 K

FIGURE 3 DEVIATIONS OF CLUSTER POPULATIONS FROM A RANDOM DISTRIBUTION AS A FUNCTION OF CONCENTRATION FOR InSbBi

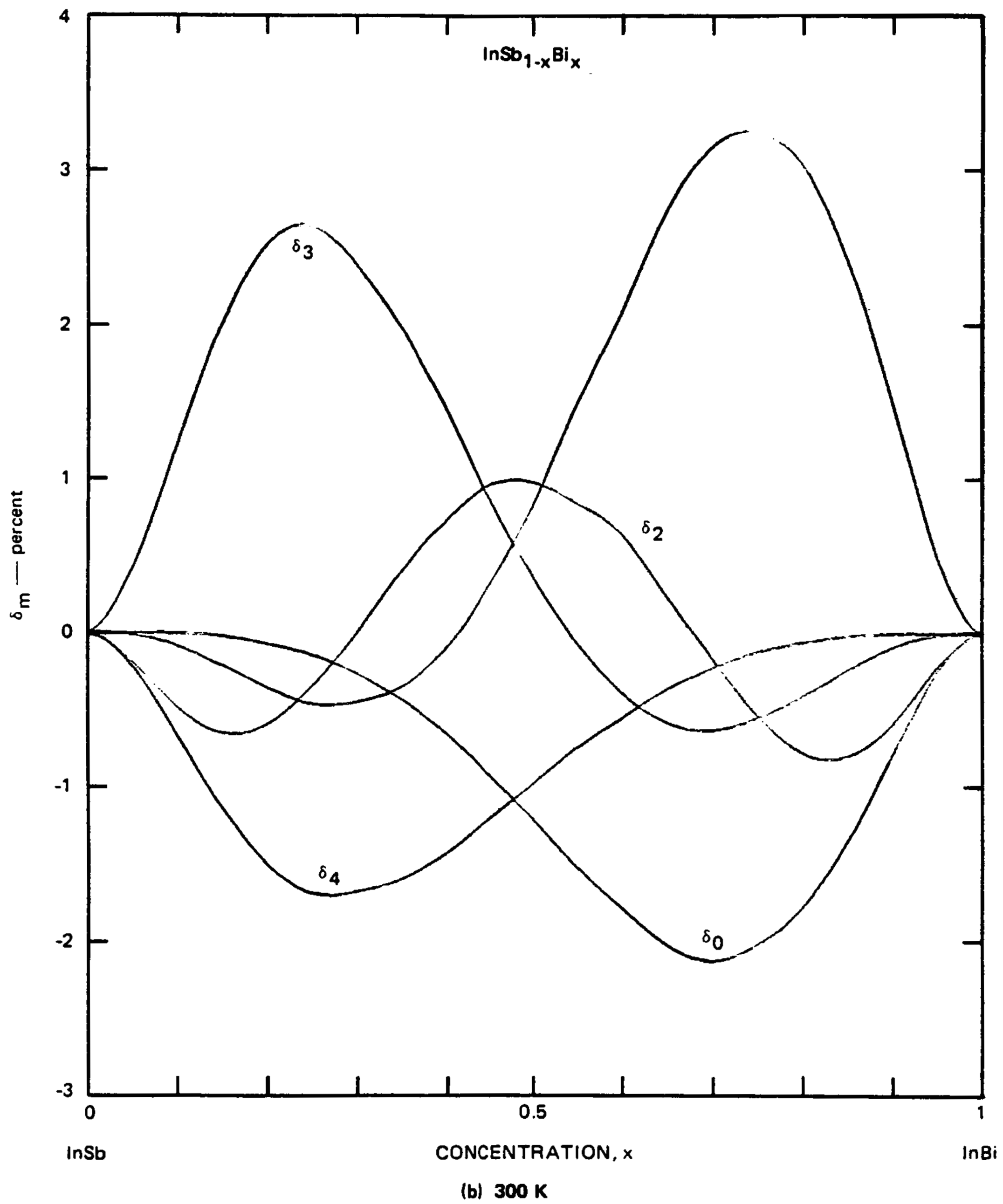

(b) 300 K

FIGURE 3 DEVIATIONS OF CLUSTER POPULATIONS FROM A RANDOM DISTRIBUTION AS A FUNCTION OF CONCENTRATION FOR InSbBi (Continued)

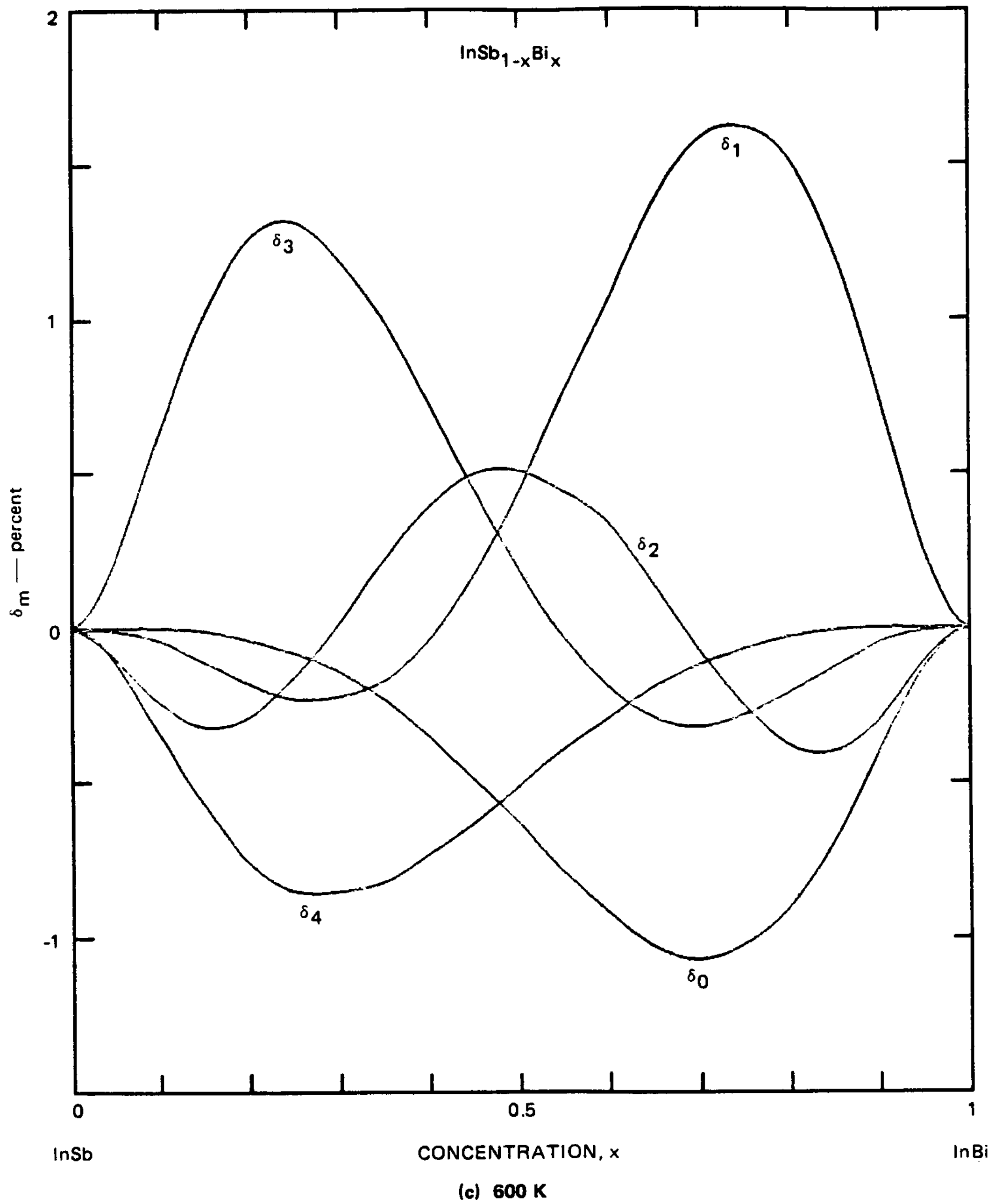

(c) 600 K

FIGURE 3 DEVIATIONS OF CLUSTER POPULATIONS FROM A RANDOM DISTRIBUTION AS A FUNCTION OF CONCENTRATION FOR InSbBi (Concluded)

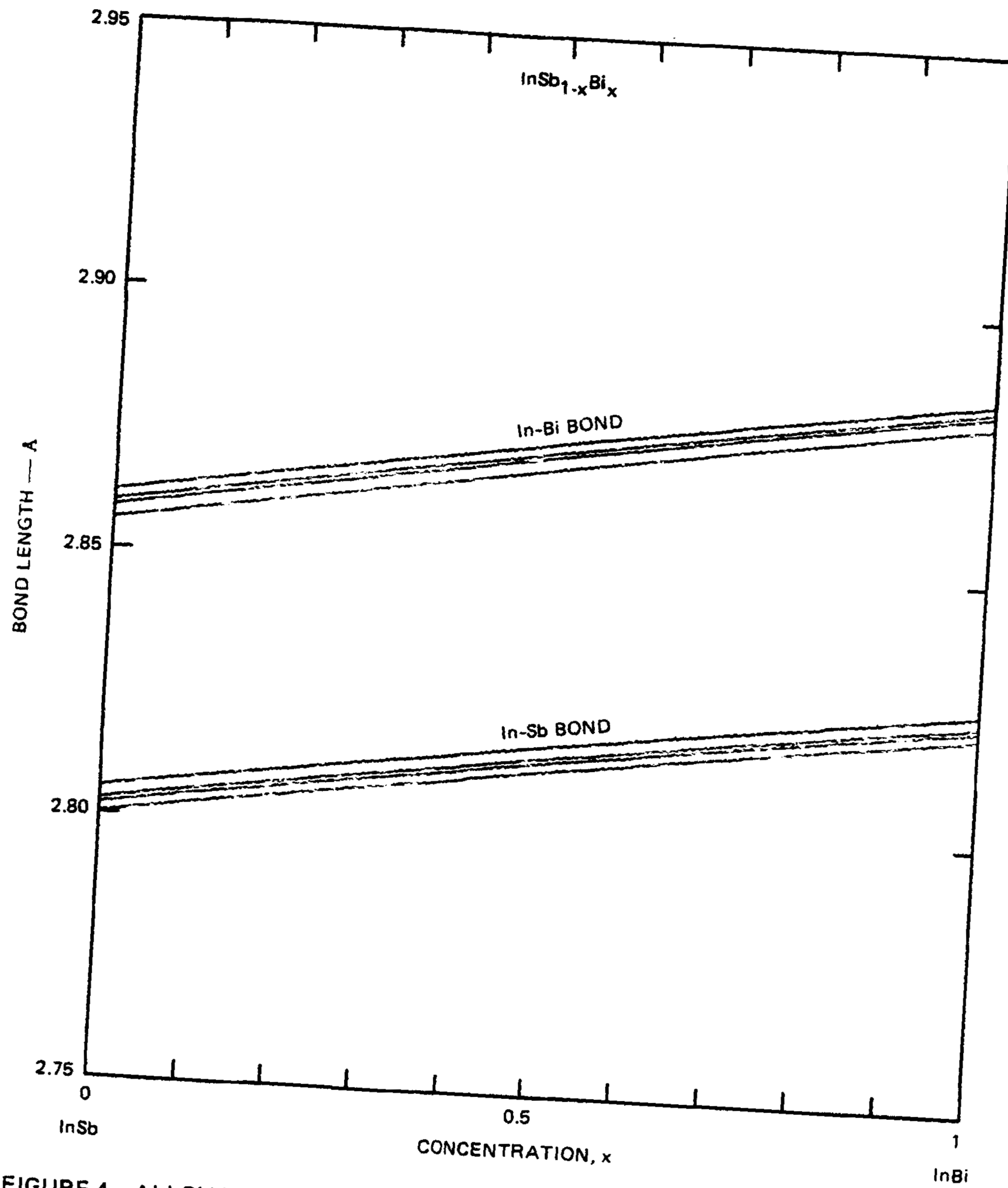

FIGURE 4 ALLOY BOND LENGTHS AS A FUNCTION OF CONCENTRATION FOR InSbBi

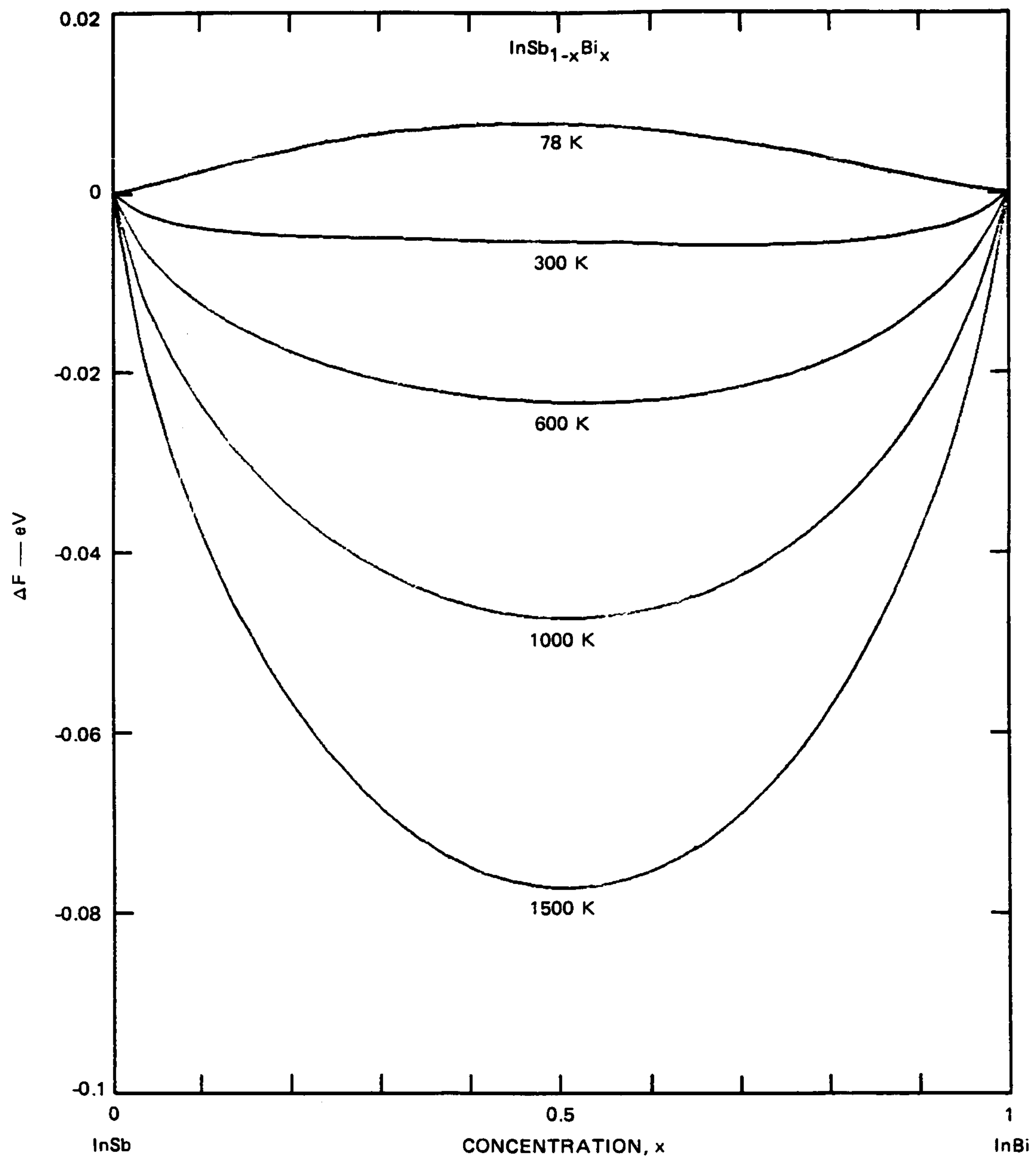

FIGURE 5 MIXING FREE ENERGIES AS A FUNCTION OF CONCENTRATION FOR InSbBi

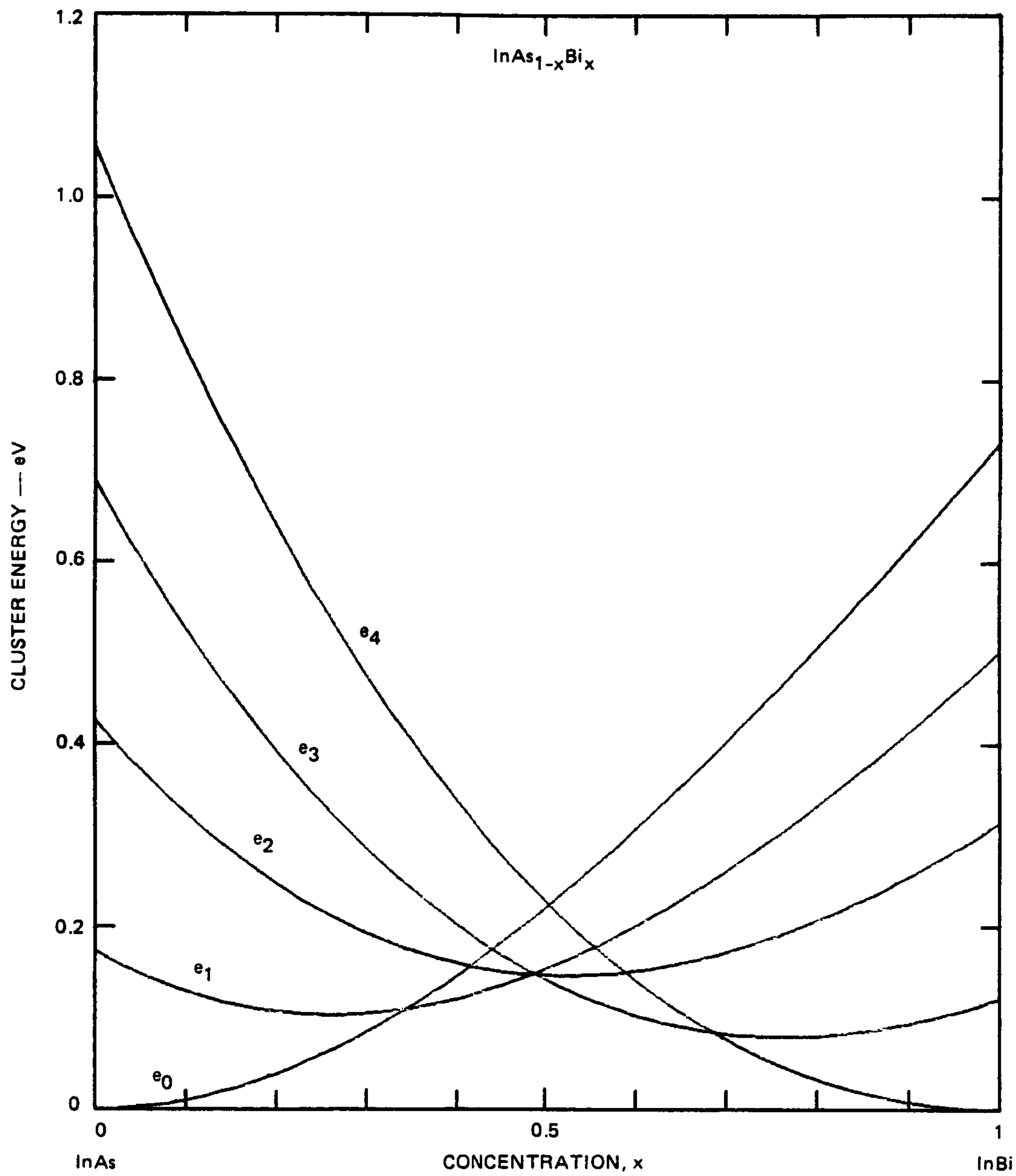

FIGURE 6 CLUSTER ENERGIES AS A FUNCTION OF CONCENTRATION FOR InAsBi

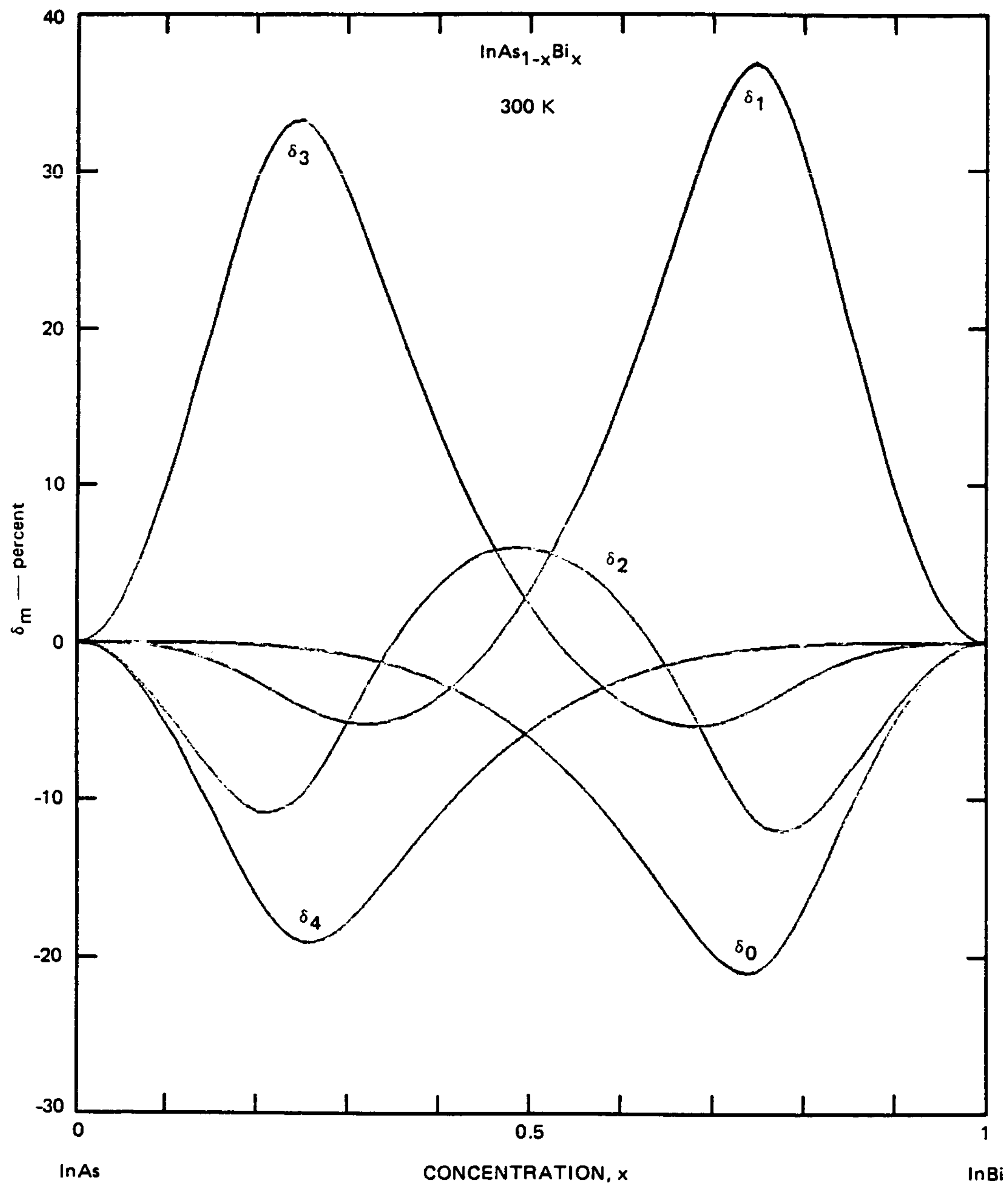

FIGURE 7 DEVIATIONS OF CLUSTER POPULATIONS FROM RANDOM DISTRIBUTIONS AS A FUNCTION OF CONCENTRATION FOR InAsBi

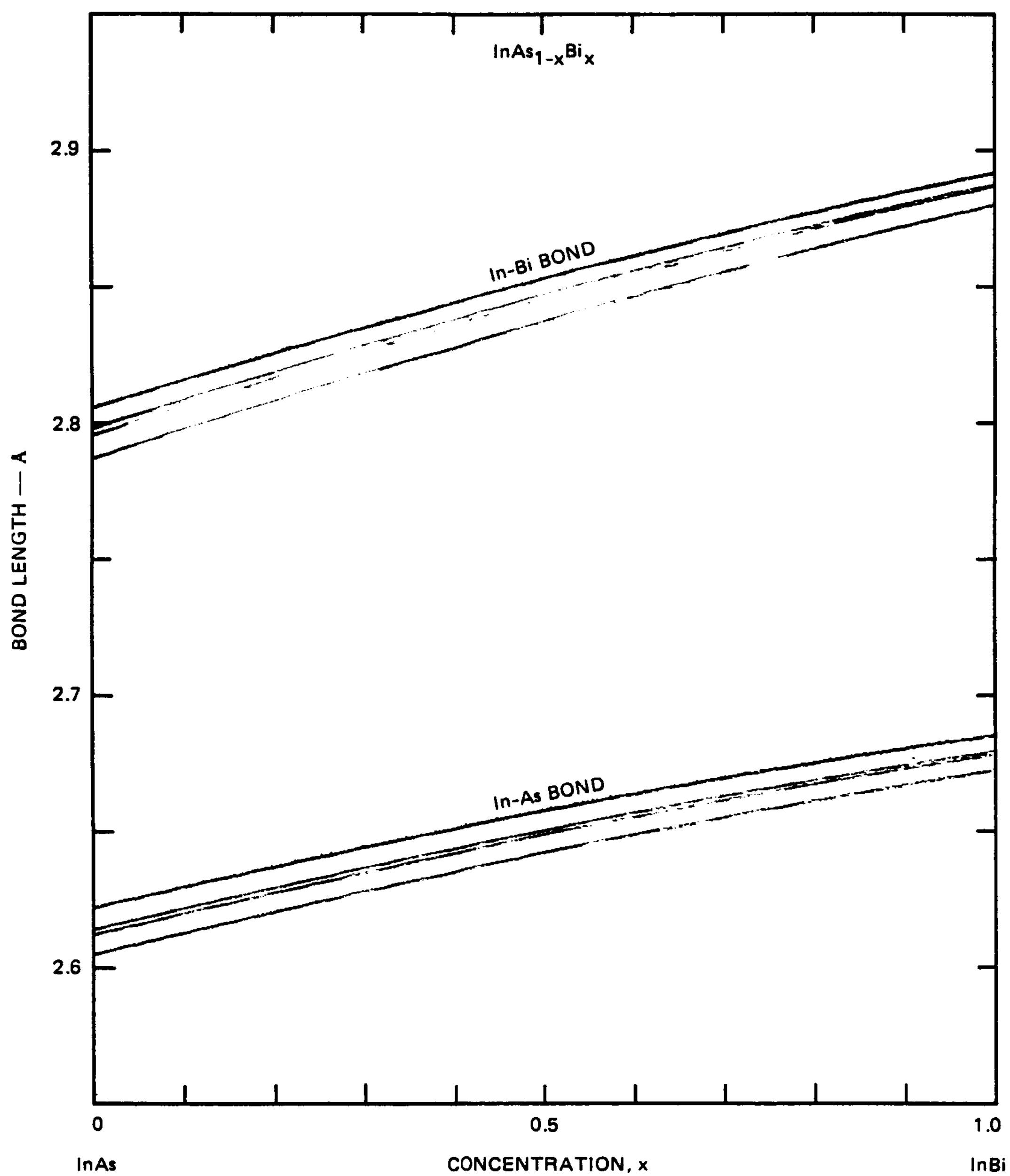

FIGURE 8 ALLOY BOND LENGTHS AS A FUNCTION OF CONCENTRATION FOR InAsBi

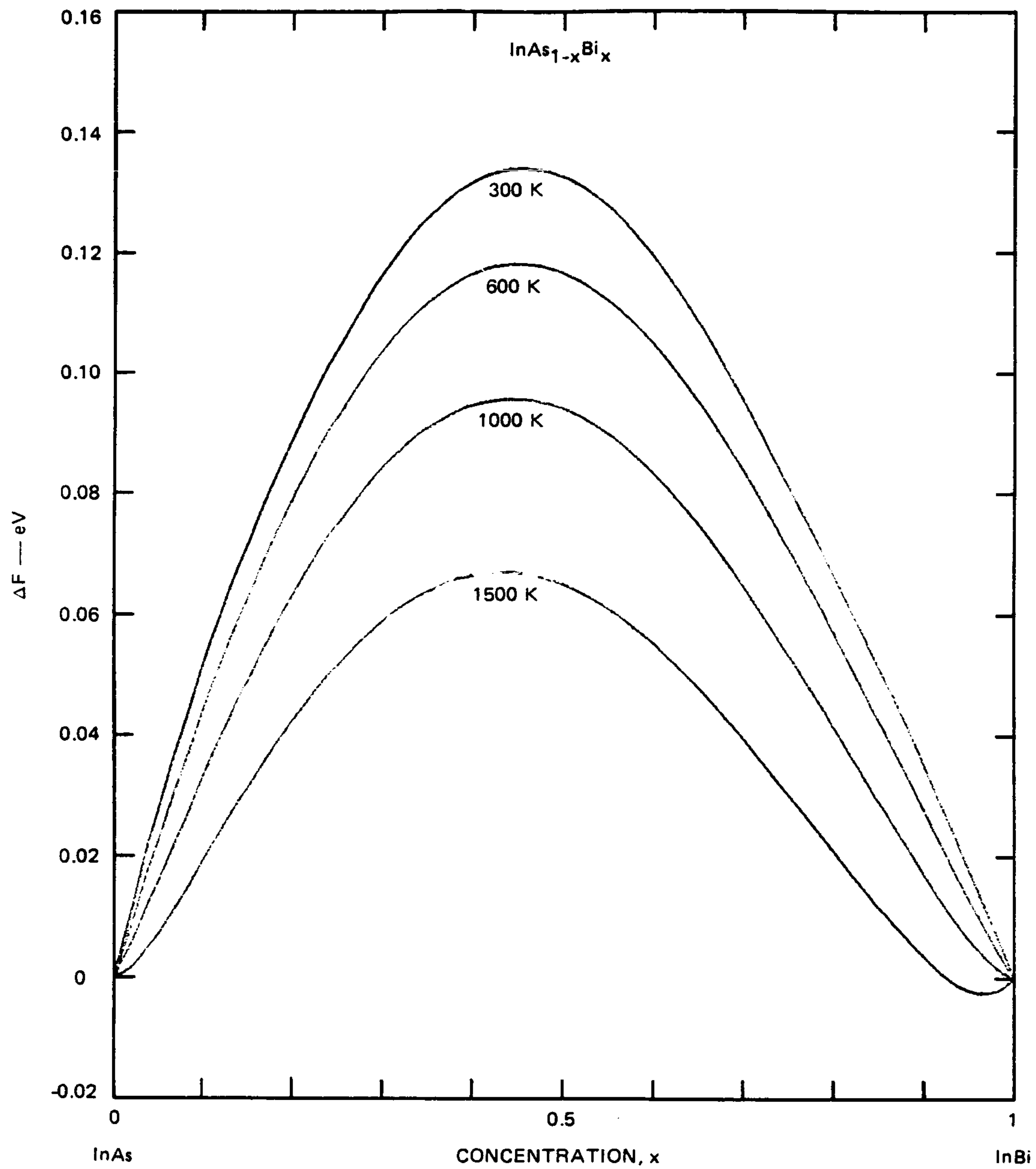

FIGURE 9 MIXING FREE ENERGY AS A FUNCTION OF CONCENTRATION FOR InAsBi

hardness from the dislocation formation energy are found to be unimportant, and contributions to the work done by the indenter by virtue of heat generation have been ignored. Sher et al. obtain the following expression for a lower limit on the hardness:

$$H_{min} = \frac{G \cot(\Theta)}{6\pi(1-\eta)} \left[-\ln\left[\frac{\cot(\Theta)}{\sqrt{2}}\right] + \frac{4}{3} + \sin^2\left[\frac{\Theta}{2}\right] \right] , \quad (16)$$

where G is the effective shear coefficient, 2Θ is the indenter tip angle, and η is Poisson ratio. In this model, the hardness is insensitive to the Burger's vector; because the hardness is dominated by the dislocation interaction terms rather than the dislocation generation terms; the hardness is also insensitive to the applied force, F, which yields a hardness that is a true property of the material.

The hardness values were computed for indium and bismuth compounds using scaled theoretical elastic constants where experimental values were not available. For an isotropic medium, $C_{44} = 0.5(C_{11} - C_{12})$; and for the effective elastic constant, G, an average of these two values was used. The results for $\Theta = \pi/4$ and $\eta = 0.2$ are summarized in Table 8.

Table 8

HARDNESS VALUES OF SEMICONDUCTORS

Compound	Effective elastic constant (10^{11} dynes/cm^2)	H_{min}, Calculated (kg/mm^2)	H, Experiment (kg/mm^2)
InP	3.71	459	467
InAs	3.19	393	353
InSb	2.28	282	213
InBi	1.98	245	—
GaBi	2.71	335	—
AlBi	2.67	329	—
GaP	5.45	673	910
GaAs	4.52	558	700
AlSb	3.01	372	343
GaSb	3.09	381	517
ZnTe	2.33	—	287
CdTe	1.24	—	154

Because the bond length of InBi is longer than that of InSb, we will expect it to diminish the hardness of the alloy; GaBi and AlBi, having shorter bond lengths, can be expected to increase the hardness of the alloys.

G. *Task 7—Vacancy Formation Energy*

The ease of vacancy formation is an important issue in the growth of materials and may influence the choice of growth methods and parameters. These energies may also significantly influence subsequent device fabrication processes. The computation of the vacancy formation energies entails several steps as outlined below:

(1) Compute the vacancy formation energy, E_v, for the pure compounds in an unrelaxed configuration.

(2) Allow relaxation about the vacancy to occur and recompute the new vacancy formation energy self-consistently, which will lower E_v.

(3) Consider various classes of clusters for a given alloy concentration to compute the alloy vacancy formation energies, including relaxation.

Here, we will be concerned only with the first step; that is, to predict the vacancy formation energies in the unrelaxed clusters for both anion and cation vacancies. The energies we will calculate will be altered by the admission of relaxation to the crystal lattice, but the values we obtained here can be considered an upper limit on E_v and will suffice to illustrate trends among compounds. We have used a simple model for calculating E_v for a neutral vacancy in a tetrahedral semiconductor such as InSbBi, based on Harrison's tight-binding theory.

As an example, consider the cation vacancy in InSb. When an In atom is removed from the crystal and put into vacuum as a neutral atom, the energy required will be the difference between the final and initial energies, $E_v = E_f - E_i$. We will consider only those energies which are changed by the vacancy formation and will include the shifts to the bonding energies out to the second-shell bonds and shifts to the metallization out to the third-shell bonds about the vacancy. The change in the energies of the first-shell bonds connecting to the dangling hybrids is primarily due to changes in the metallization energy. However, because the hybrid energy ε_h is very close to the bond energy, ε_b, we cannot use the perturbation theory for these energy shifts in the final state cluster.

If the second-neighbor interactions are not included, the dangling hybrids are not interacting with each other. We can then treat each of the four branches associated with each dangling hybrid separately. To avoid the error in the perturbation theory, we diagonalize a local Hamiltonian H for each branch. This H is spanned by seven hybrids: the dangling one, the three connecting to this one and sharing the common anion (and interacting with each other via V_{1a}), and the three cation hybrids which face the last three anion hybrids and interact with them via V_2:

$$\varepsilon_h^a = (\varepsilon_s^a + \varepsilon_{p1/2}{}^a + 2\varepsilon_{p3/2}{}^a)/4 \tag{17}$$

$$\varepsilon_h{}^c = (\varepsilon_s{}^c + \varepsilon_{p1/2}{}^c + 2\varepsilon_{p3/2}{}^c)/4 \tag{18}$$

$$V_2 = -24.5/d^2 \tag{19}$$

$$V_1^a = (\varepsilon_s^a - \varepsilon_p^a)/4 \tag{20}$$

$$V_1^c = (\varepsilon_s^c - \varepsilon_p^c)/4 \quad . \tag{21}$$

Diagonalization of this 7×7 Hamiltonian yields seven modified energies, ε_i, i from 1 to 7. The first three are the modified bond energies, which should be occupied by two electrons each. The fourth level corresponds to the modified dangling hybrid energy which, for the cation vacancy in a III-V compound such as InSb, is occupied by 5/4 electrons per level. The fifth through seventh states are unoccupied antibonding states.

In our model, the energies of the bonds outside the 7×7 cluster are not changed to first order. The shift in the bond energies resulting from the diagonalization of the 7×7 does cause a shift in the metallization interaction between the antibonding states localized in the 7×7 cluster and the adjacent bonds outside the cluster. Similarly, the metallization interaction of the cluster bonding states with the outer antibonding states is modified.

The energy of the final state cluster, E_f, for a cation vacancy in a III-V compound is given by (keeping track of only those terms which change upon formation of a vacancy)

$$E_f = \varepsilon_{atom} + 5\varepsilon_4' + 4 \times 2\,(\varepsilon_1' + \varepsilon_2' + \varepsilon_3') \tag{22}$$

$$+ 2 \times 4 \times 3\,(\varepsilon_{met,4} + \varepsilon_{met,5} + \varepsilon_{met,6} + \varepsilon_{met,7}) \quad ,$$

where ε_{atom} is the valence electron energy of the free atom, and ε_1', ε_2', ε_3', and ε_4' are the cluster bond energies, which have been shifted by the metallization with the third-shell antibonds,

$$\varepsilon_i' = \varepsilon_i + 3\varepsilon_{mi} \quad , \tag{23}$$

$$\varepsilon_{mi} = \frac{|V_1^c|^2\,|U_a^c|^2}{\varepsilon_i - \varepsilon_a} \sum_j |U_{ji}|^2 \quad ,$$

where j sums over the three second-shell hybrids which connect to the third shell. The $\varepsilon_{met,i}$ are the shifts in the third-shell bond energies due to the interaction with the bonding states of the 7×7 cluster:

$$\varepsilon_{met,i} = \frac{|V_1^c|^2\,|U_b^c|^2}{\varepsilon_b - \varepsilon_i} \sum_j |U_{ji}|^2 \quad , \tag{24}$$

where the j summation is as in Eq. (23). For the initial state energy, E_i, we have

$$E_i = \varepsilon_b' + 4V_0 + 4 \times 2\,(\varepsilon_b' + \varepsilon_b' + \varepsilon_b') \qquad (25)$$

$$+ 2 \times 4 \times 3 \times 3\,(\varepsilon_m^c) \quad ,$$

where ε_b' is the bonding state energy which has been shifted because of metallization through the anion and the cation sites:

$$\varepsilon_b' = \varepsilon_b + 3\varepsilon_m{}^c + 3\varepsilon_m{}^a \quad , \qquad (26)$$

$$\varepsilon_m{}^c = \frac{|V_1{}^c|^2\,|U_a{}^c|^2\,|U_b{}^c|^2}{\varepsilon_b - \varepsilon_a} \quad , \qquad (27)$$

and similarly for $\varepsilon_m{}^a$. V_0 is the repulsive energy of the four central bonds that will be broken upon the creation of the vacancy.

The four eigenvalues localized on the dangling hybrids are degenerate, because there are no couplings between the four branches of the cluster when no dangling hybrid interactions are included. When these couplings are included, the dangling hybrid states are split into one A_1 and three T_2 triply degenerate states, according to the Td point symmetry of the vacancy site. The degeneracy of the three T_2 states can further split when the cluster is permitted to relax in the presence of strain energies.

The vacancy formation energy is computed as the energy necessary to remove an atom from the perfect lattice to infinity, here assuming no lattice relaxation occurs. The vacancy formation energy will, in general, differ for the anion and the cation. We assume that the changes of the bond energies neighboring the vacancy will be adequately described by the bonds that we have considered. Thus, the vacancy formation energy E_v is computed from the difference

$$E_v = E_f - E_i \quad . \qquad (28)$$

The vacancy formation energies are summarized in Table 9.

Table 9

VACANCY FORMATION ENERGIES FOR Bi COMPOUNDS AND OTHER GROUP IV, III-V, AND II-VI COMPOUNDS*

Compound	Vacancy Formation Energy (eV)*							
	Anion Vacancy				Cation Vacancy			
	E_{v1}	E_{v2}	E_{v3}	E_v	E_{v1}	E_{v2}	E_{v3}	E_v
C	0.00	0.00	0.00	0.00	36.75	-3.63	-0.38	32.75
Si	0.00	0.00	0.00	0.00	16.87	-4.68	-1.33	10.86
Ge	0.00	0.00	0.00	0.00	18.03	-7.07	-30.2	7.95
Sn	0.00	0.00	0.00	0.00	15.12	-6.59	-3.27	5.25
AlP	13.29	-1.12	-2.21	9.96	23.81	-11.71	-0.16	11.93
AlAs	12.34	-1.14	-3.46	7.74	24.20	-13.45	-0.13	10.61
AlSb	10.94	-1.75	-4.61	4.57	18.96	-11.25	-0.22	7.49
AlBi	12.16	-1.66	-7.64	2.86	20.79	-13.38	-0.16	7.24
GaP	12.98	-2.23	-3.78	6.96	21.92	-11.74	-0.29	9.89
GaAs	12.53	-2.34	-5.92	4.28	22.28	-13.65	-0.25	8.38
GaSb	12.16	-3.40	-7.03	1.72	17.40	-11.47	-0.43	5.50
GaBi	14.28	-3.35	-11.24	-0.32	19.09	-13.89	-0.36	4.84
InP	11.00	-1.49	-3.79	5.71	22.61	-13.01	-0.13	9.47
InAs	10.54	-1.54	-5.86	3.14	23.01	-14.89	-0.08	8.04
InSb	10.07	-2.37	-7.56	0.15	17.94	-12.57	-0.15	5.22
ZnTe	8.66	-0.67	-2.69	5.31	20.08	-14.91	-0.04	5.14
HgTe	7.37	-1.17	-5.31	0.90	17.97	-15.64	-0.02	2.31
CdTe	7.66	-0.48	-2.50	4.69	20.43	-15.56	-0.01	4.86

*E_{v1}, E_{v2}, and E_{v3} refer to contributions to the total energy, E_v, from the first, second, and third shells.

III CONCLUSIONS

All three of the bismuth compounds AlBi, GaBi, and InBi show negative bonding energies from -1.2 to -1.6 eV, indicating that, if made, the zincblende structures would be bound and perhaps more strongly bound than the II-VI compounds currently used for infrared detection devices. No calculations were done for structures other than zincblende for the Bi compounds, although the large spin-orbit splitting in Bi, which results in a large promotion energy in the bond energy, and the lack of experimental observation of zincblende Bi compounds indicate that the zincblende structure is not the lowest energy state for the binary systems. Because of the negative binding energy of all of the Bi compounds, all three can be considered candidates for alloying with other III-V compounds for narrow-gap semiconductors.

None of the bismuth compounds are known to form zincblende structures, so none of the cation-substituted alloys are deemed likely to form even reasonably metastable zincblende structures. Thus, without a stable III-V compound as one alloy component, the anion-substituted alloys AlGaBi, AlInBi, and GaInBi are not considered strong candidates for growth as narrow-gap semiconductors. The anion-substituted alloys however, are more promising.

Zilko and Green (1978; 1980) found the semimetal-semiconductor transition occurring at ~ 11 mole percent in the metastable InSbBi. Assuming little band-gap bowing in the alloys, such that the band gap as a function of concentration, x, is approximately a straight line, a band gap of -1.5 eV is extrapolated for the semimetal zincblende InBi. Assuming little band gap bowing for all Bi alloys, we find the following approximate concentrations, x, to achieve a band gap of 0.1 eV:

Alloy	*X*
$InP_{1-x}Bi_x$	0.44
$InAs_{1-x}Bi_x$	0.14
$InSb_{1-x}Bi_x$	0.05

Alloy hardening is observed in the zincblende semiconductors, where the hardness as a function of concentration x shows an upward bowing relative to the straight-line average. Because hardness depends on the inverse of the bond length to some power, alloying a compound such as InP, InAs, or InSb with a longer-bond-length compound such as InBi may result in an alloy which is harder than the constituents. For a material with a band gap of 0.1 eV, one expects the hardest material from InPBi, the least hard from InSbBi. Thus, even though more than 40 percent Bi in InP is needed to achieve the desired band gap, the alloy hardening will result in a hard material, harder than the currently favored narrow-gap alloy HgCdTe. In comparison, a 0.1 eV alloy of InSbBi will be a relatively soft material, of comparable structural quality to HgCdTe. Thus, based on the predicted structural properties, InPBi, if it can be grown at all, appears the most promising candidate for infrared device materials.

PRECEDING PAGE BLANK NOT FILMED

The results of the miscibility calculations indicate that InSbBi will be the easiest of the anion-substituted alloys to grow, having the smallest bond length mismatch. A range of miscibility for InPBi and InAsBi exists at high temperatures. For InPBi, the results of the dilute alloy calculation indicate that InP and InBi has a miscibility gap, because the melting temperature of InP is lower than the critical temperature. The results of the cluster calculations indicate that even InAsBi (with a lattice mismatch of ~ 9 percent compared to ~ 13 percent for InPBi) will be hard to mix, because the lattice mismatch of the constituents.

Thus to grow the structurally superior InPBi alloy, one must resort to nonequilibrium growth methods, such as energy-assisted epitaxy employed by Zilko and Green (1978, 1980), where the effective growth temperature is kept high. By growing the alloy at an elevated temperature, one can achieve a regime of constituent miscibility. Although our results indicate that InPBi may be immiscible, if it is miscible only at elevated temperatures (~ 1300 K), its promise to be a structurally superior narrow-gap semiconductor justifies a program for growth of this alloy. Because of the smaller bond length mismatch of their constituents, InAsBi and InSbBi shows less tendency toward immiscibility than InPBi. Unfortunately, InAsBi and InSbBi will probably be less hard than InPBi and of comparable hardness to HgCdTe, thus reducing the incentive for growth of these materials.

REFERENCES

American Institute of Physics Handbook, 1972: 3rd ed., edited by D.E. Gray (McGraw-Hill, New York), pp. 9-16.

Bachelet, G.B., D.R. Hamann, and M. Schlüter; "Pseudopotentials That Work: From H to Pu," *Phys. Rev. B, 26*, p. 4199.

Chen, A.-B., and A. Sher, 1983: "Bonding Theory of Semiconductor Alloys," *Microscience, 3*, p. 1.

Chen, A.-B., and A. Sher, 1985a: "Semiconductor Pseudobinary Alloys: Bond Length Relaxation and Mixing Enthalpies," *Phys. Rev. B, 32*, p. 3695.

Chen, A.-B., and A. Sher, 1985b: "Semiconductor Alloys: Local Bond Lengths, Mixing Enthalpies, and Microclusters," *Mat. Res. Soc. Symp. Proc., 46*, p. 137.

Harrison, W., 1980: *Electronic Structure and Properties of Solids* (Freeman, San Francisco).

Harrison, W., 1983: "The Bonding Properties of Semiconductors," *Microscience, 3*, p. 35 [a multiclient publication of SRI International, Menlo Park, California].

Jean-Louis, A.M., and C. Hamon, 1969a: "Propriétés des Alliages $InSb_{1-x}Bi_x$; I. Measures Électriques," *Phys. Stat. Sol., 34*, p. 329.

Jean-Louis, A.M., B. Ayrault, and J. Vargas, 1969b: "Propriétés des Alliages $InSb_{1-x}Bi_x$; II Absorption Optique," *Phys. Stat. Sol., 34*, p. 341.

Joukoff, B., and A.M. Jean-Louis, 1972: "Growth of $InSb_{1-x}Bi_x$ Single Crystals by Czochralski Method," *J. Cryst. Growth, 12*, p. 169.

Keating, P., 1966: "Effect of Invariance Requirements on the Elastic Strain Energy of Crystals with Application to the Diamond Structure," *Phys. Rev., 145*, p. 636.

Martin, R., 1970: "Elastic Properties of ZnS Structure Semiconductors," *Phys. Rev. B, 10*, p. 4005.

Noreika, A.J., W.J. Takei, M.H. Francombe, and C.E.C. Wood, 1982: "Indium Antimonide-Bismuth Compositions Grown by Molecular Beam Epitaxy," *J. Appl. Phys., 53*, p. 4932.

Noreika, A.J., J. Greggi, W. Takei and M.H. Francombe, 1983: "Properties of MBE Grown InSb and $InSb_{1-x}Bi_x$," *J. Vac. Sci. Technol., A-1*, p. 558.

Oe, K., S. Ando, and K. Sugiyama, 1981: ''$InSb_{1-x}Bi_x$ Films Grown by Molecular Beam Epitaxy,'' *Jap. J. Appl. Phys., 20*, p. L303.

Sher, A., A.-B. Chen, W.E. Spicer, and C-K Shih, 1985a: ''Effects Influencing the Structural Integrity of Semiconductors and Their Alloys,'' *J. Vac. Sci. Technol., A3*, p. 105.

Sher, A., A.-B. Chen, and W.E. Spicer, 1985b: ''Dislocation Energies and Hardness of Semiconductors,'' *Appl. Phys. Lett., 46*, p. 54.

Wyckoff, R., 1963: *Crystal Structures*, Vol. 1 (J. Wiley, New York).

Zilko, J. and J. Greene, 1978: ''Growth of Metastable $InSb_{1-x}Bi_x$ Thin Films by Multitarget Sputtering,'' *Appl. Phys. Lett., 33*, p. 254.

Zilko, J. and J. Greene, 1980: ''Growth and Phase Stability of Epitaxial Metastable $InSb_{1-x}Bi_x$ Films on GaAs. I. Crystal Growth. *J. Appl. Phys., 51*, p. 1549.

1. Report No.
NASA CR-4030

2. Government Accession No.

3. Recipient's Catalog No.

4. Title and Subtitle
STRUCTURAL PROPERTIES OF BISMUTH-BEARING SEMICONDUCTOR ALLOYS

5. Report Date
DECEMBER 1986

6. Performing Organization Code

7. Author(s)
Martha A. Berding, A. Sher, and A.-B. Chen

8. Performing Organization Report No.
SRI Project 1452

9. Performing Organization Name and Address
SRI International
333 Ravenswood Avenue
Menlo Park, California 94025

10. Work Unit No.

11. Contract or Grant No.
NAS1-18180

12. Sponsoring Agency Name and Address
National Aeronautics and Space Administration
Washington, D.C. 20546

13. Type of Report and Period Covered
Contractor Report

14. Sponsoring Agency Code
506-54-23-13

15. Supplementary Notes
Martha A. Berding and A. Sher: SRI International, Menlo Park, California.
A.-B. Chen: Auburn University, Auburn, Alabama.
Langley Technical Monitor: W.E. Miller
Final Report

16. Abstract

We have addressed the structural properties of bismuth-bearing III-V semiconductor alloys. Because the Bi compounds are not known to form zincblende structures, only the anion-substituted alloys InPBi, InAsBi, and InSbBi are considered candidates as narrow-gap semiconductors. Miscibility calculations indicate that InSbBi will be the most miscible, and InPBi, with the large lattice mismatch of the constituents, will be the most difficult to mix. Calculations of the hardness of the Bi compounds indicate that, once formed, the InPBi alloy will be harder than the other Bi alloys, and substantially harder than the currently favored narrow-gap semiconductor HgCdTe. Thus, although InSbBi may be an easier material to prepare, InPBi promises to be a harder material. Growth of the Bi compounds will require high effective growth temperatures, probably attainable only through the use of nonequilibrium energy-assisted epitaxial growth techniques.

17. Key Words
Bismuth, Alloys, Semiconductors,
Narrowgap Semiconductors

18. Distribution Statement
Unclassified–Unlimited
Subject Category 76

19. Security Classif. (of this report)	20. Security Classif. (of this page)	21. No. of Pages	22. Price
Unclassified	Unclassified	42	A03

*For sale by the National Technical Information Service, Springfield, Virginia 22161

NASA-Langley, 1986